Synthetic pluripotent bacterial stem cells

Sara Molinari[1,*], David L. Shis[1,*], James Chappell[1], Oleg A. Igoshin[1,2,3], Matthew R. Bennett[1,2,†].

[1] Department of Biosciences, Rice University, Houston, TX

[2] Department of Bioengineering, Rice University, Houston, TX

[3] Center for Theoretical Biological Physics, Rice University, Houston, TX

[*] Equal contribution

[†] Correspondence: matthew.bennett@rice.edu

Abstract

A defining property of stem cells is their ability to differentiate via asymmetric cell division, in which a stem cell creates a differentiated daughter cell but retains its own phenotype. Here, we describe a synthetic genetic circuit for controlling asymmetrical cell division in *Escherichia coli*. Specifically, we engineered an inducible system that can bind and segregate plasmid DNA to a single position in the cell. Upon division, the co-localized plasmids are kept by one and only one of the daughter cells. The other daughter cell receives no plasmid DNA and is hence irreversibly differentiated from its sibling. In this way, we achieved asymmetric cell division though asymmetric plasmid partitioning. We also characterized an orthogonal inducible circuit that enables the simultaneous asymmetric partitioning of two plasmid species – resulting in pluripotent cells that have four distinct differentiated states. These results point the way towards engineering multicellular systems from prokaryotic hosts.

Introduction

Synthetic biology enables fundamental studies of biology[1,2] and the construction and characterization of genetic systems from the ground up[3–5]. Long used for the task of expressing recombinant proteins, synthetic organisms now hold promise for more complex applications[6] such as targeting tumors[7], drug discovery[8], biopharmaceutical production[9,10], antibiotic and gene therapies[11,12], microbiome manipulation[13], and geoengineering[14]. However, synthetically engineered bacterial systems are relatively simple compared to complex multicellular systems that exist in nature. While some synthetic bacteria can produce population-scale behaviors such as pattern formation[15–18], robust synchronized oscillations[19–21], and growth rate control[22], no synthetic bacteria can compare to the highly coordinated activities of multicellular organisms.

One of the primary methods found in nature for creating complex spatially distributed systems is cellular differentiation via the process of asymmetric cell division. Asymmetric cell

division enables the development of different cell types within the organism to specialize by partitioning biochemical or physical tasks throughout the body within tissues and organs. In multicellular eukaryotes, cellular differentiation is generally achieved through complex regulatory networks that utilize transcriptional regulation, post-transcriptional modifications, and chromatin remodeling. To differentiate asymmetrically, a progenitor cell type (such as a stem cell) senses chemical cues in the environment to alter the transcriptional landscape in the daughter cell. This transcriptional rearrangement of the daughter cell is complete enough that de-differentiation is rare and reproducible in the lab only through the very specific and simultaneous induction of many genes[23].

Cellular differentiation is not a purely eukaryotic phenomenon. Indeed, many types of bacteria can also undergo limited forms of asymmetric cellular differentiation. For example, the soil bacterium *Bacillus subtilis* possesses a wide variety of environmental sensing/response systems that, when nutrients are scarce, initiate either a unicellular (sporulation) or a multicellular (biofilm) differentiation program[24–27]. Within biofilms, cells further differentiate spatially with different cell types localizing in distinct regions within the biofilm[28,29]. In other bacterial genera, differentiation between non-motile and motile cells can allow cells to achieve coordinated population migration[30–32]. In some microbes, every cell cycle can produce two distinct cell types. For instance, in *Caulobacter crescentus*, each cell division leads to the formation of a swarmer cell that moves around exploring the environment and a stalked cell that stays attached to a substrate[33,34].

Several attempts have been made to create synthetic bacteria that have multiple stable transcriptional profiles[3,35]. The first of these was the co-repressive toggle switch in *E. coli* designed by Gardner and colleagues[3]. Essentially, this synthetic genetic circuit contains the genes encoding for two transcriptional repressors, *lacI* and *tetR*, each driven by a promoter that is repressed by the others' protein product. The authors found that gene expression was

bimodal for cells containing this circuit – cells either had high levels of LacI and low levels of TetR, or, conversely, low levels of LacI and high levels of TetR. The co-repressive toggle switch achieves cellular differentiation in a manner similar to stem cells– *i.e.* through the rearrangement of the transcriptional landscape. However, the regulatory network in the co-repressive toggle is much simpler than those found in high-ordered eukaryotes, which utilize multiple redundant regulatory processes to quench unwanted transitions between cell types. Indeed, the co-repressive toggle is very sensitive to intrinsic and extrinsic sources of gene regulatory noise[3,36–39], and can only transiently maintain one state before stochastically switching back to the other.

To create asymmetric cell division in *E. coli*, we refactored two key elements of the chromosome partitioning system of *C. crescentus*[40] into *E. coli*. The *par* system is ubiquitous in many organisms and is principally responsible for the segregation of low copy number plasmids or chromosomes. They all share a similar mechanism: the initial pairing of the plasmids/chromosomes through the binding of a centromere-like *cis*-acting sequence (a *parS* region) by a centromere-binding *trans*-acting protein (a ParB like protein) leading to the formation of a large nucleoprotein complex[41]. For the symmetric segregation of DNA to be successful, a motor protein is also required to shuttle the chromosomes to opposite poles[41,42].

In this study, we show that by refactoring the *par* system from *C. crescentus* one can control the asymmetric partitioning of plasmid DNA. Accumulation of ParB gathers plasmid DNA containing a *parS* site into a single cluster within the cell. The single DNA/protein complex then partitions into one and only one of the daughter cells upon cell division. This creates two cell types: “progenitor cells”, cells that have retained plasmid DNA, and “differentiated cells,” cells that did not inherit plasmid DNA. We show that progenitor cells can give rise to multiple rounds of differentiation and that many types of plasmids may be targeted. We further show that refactoring the *par* system from the F plasmid facilitates an orthogonal pathway for inducible

asymmetric plasmid partitioning (APP). Using these two pathways, we engineered a synthetic genetic circuit that imparts pluripotency to the host cells – i.e. two different plasmids can be independently partitioned asymmetrically to create four distinct cell types. This new technology will allow synthetic biologists to create large-scale multicellular bacterial communities that can differentiate from a single cell.

Results

APP in *E. coli*

The circuit we constructed for APP in *E. coli* is illustrated in Fig. 1a. It consists of two elements of the *par* operon from *C. crescentus*: the centromere-like site *parS* and the centromere-binding protein encoded by *parB*[40]. We cloned the *cis*-acting *parS* sequence, which contains two sites for the specific binding of ParB dimer[40], onto a plasmid that we refer to as the "target plasmid." On a second plasmid, which we call the "regulatory plasmid" we cloned the gene encoding ParB fused to super folder yellow fluorescent protein (sfYFP) under the control of an arabinose-inducible promoter. When present, ParB binds to *parS* and forms a nucleoprotein complex surrounding the *parS* site through a combination of homodimerization interactions and non-specific binding of ParB to DNA around *parS*[43,44] This characteristic of ParB consolidates copies of the target plasmid[41] into a single cluster as shown in Fig. 1b. Upon induction of the system, one daughter cell ultimately inherits the nucleoprotein oligomer, facilitating the asymmetric partitioning of the target plasmid. The other septation partner loses the target plasmid and becomes terminally differentiated. In this way, asymmetrical cell division happens through APP (Fig. 1c).

To characterize the induction of APP, we first utilized single cell fluorescence microscopy by tracking the nucleoprotein complex around the *parS* sequence, which appears as a yellow fluorescent punctum. To track the segregation of target plasmid DNA, we cloned a

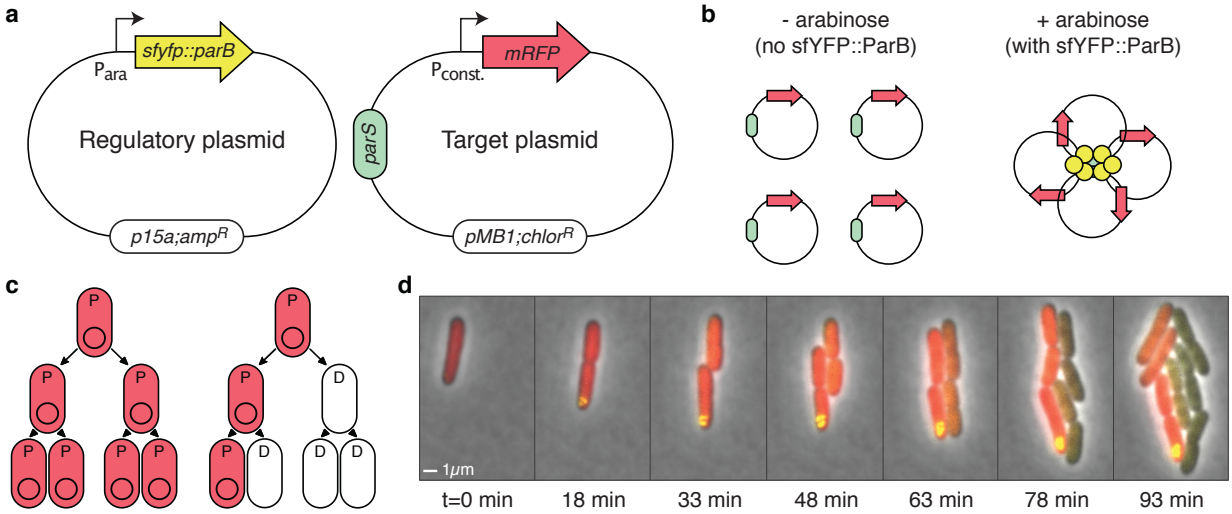

Figure 1 Asymmetric plasmid partitioning in *E. coli*. **(a)** The APP network consists of two plasmids: the regulatory plasmid containing *parB* under the control of an arabinose inducible promoter and the target plasmid containing the *parS* sequence and the gene encoding red fluorescent protein. **(b)** In the absence of arabinose (left), there is no ParB, so target plasmids are free to diffuse around the cell. However, when arabinose is present (right), ParB binds the *parS* sequence on the target plasmid, forming a nucleoprotein complex that gathers all copies of the plasmid together. **(c)** At the population level, target plasmids segregate normally in the absence of arabinose (left) and all cells remain progenitor cells (denoted by "P"). Upon induction (right), progenitor cells begin to asymmetrically divide, giving rise to daughter cells (denoted by "D"). Note that, during induction, daughter cells are free to propagate, while the number of progenitor cells should remain constant. **(d)** Time-lapse fluorescence microscopy of cells undergoing asymmetric plasmid partitioning. Shown at time t=0 is a single progenitor cell that is in the presence of arabinose. A nucleoprotein complex quickly forms (yellow punctum), and subsequent daughter cells lose the target plasmid. The inherited red fluorescent protein in the daughter cells quickly decays through dilution and proteolysis.

gene encoding a proteolytically tagged red fluorescent protein (mRFP) onto the target plasmid and followed the proliferation of red fluorescence in a population of dividing cells. Cells transformed with both the regulatory plasmid and the target plasmid were cultured on an agar pad perfused with arabinose and imaged over time (see Methods). At the beginning of cell growth, several small florescent foci formed inside the cells at apparently random positions; these foci then segregated randomly to both daughter cells (Fig. S1). This correlates with the observation that both daughter cells retain red fluorescence, suggesting inheritance of target plasmid DNA. However, as the puncta of YFP fluorescence become larger and consolidate, segregation of the nucleoprotein complex to only one daughter cell upon cell division becomes the norm. In this case, red fluorescence tightly correlates with the presence of a single punctum of YFP fluorescence. The presence of fluorescent puncta suggests the presence of the target plasmid inside the cell (Fig. S2). The loss of fluorescent puncta hence suggests that the cell has lost target plasmid DNA. In agreement with this hypothesis, single cell microscopy shows that daughter cells that do not inherit the fluorescent puncta (and presumably the plasmid-ParB complex) also rapidly degrade the red fluorescence signal. Furthermore, once red fluorescence was lost, we never observed it to be recovered. This contrasts with the maintenance of red fluorescence in cells that retain YFP fluorescence. A representative example of this process is shown in Fig. 1d.

In addition to single cell fluorescence microscopy, we also tracked the proliferation of target plasmid DNA in populations by first growing them in flask (with or without arabinose) and then plating them onto LB agar plates (with or without chloramphenicol, the selective antibiotic for target plasmid), as depicted in Fig. 2a (see Methods). In the absence of arabinose, APP does not occur, so target plasmid DNA segregates normally. Hence, chloramphenicol resistance is present in every cell, and the number of colony forming units (CFUs) at each stage of growth does not depend on the presence or absence of chloramphenicol in the plate (Fig. 2b, black and

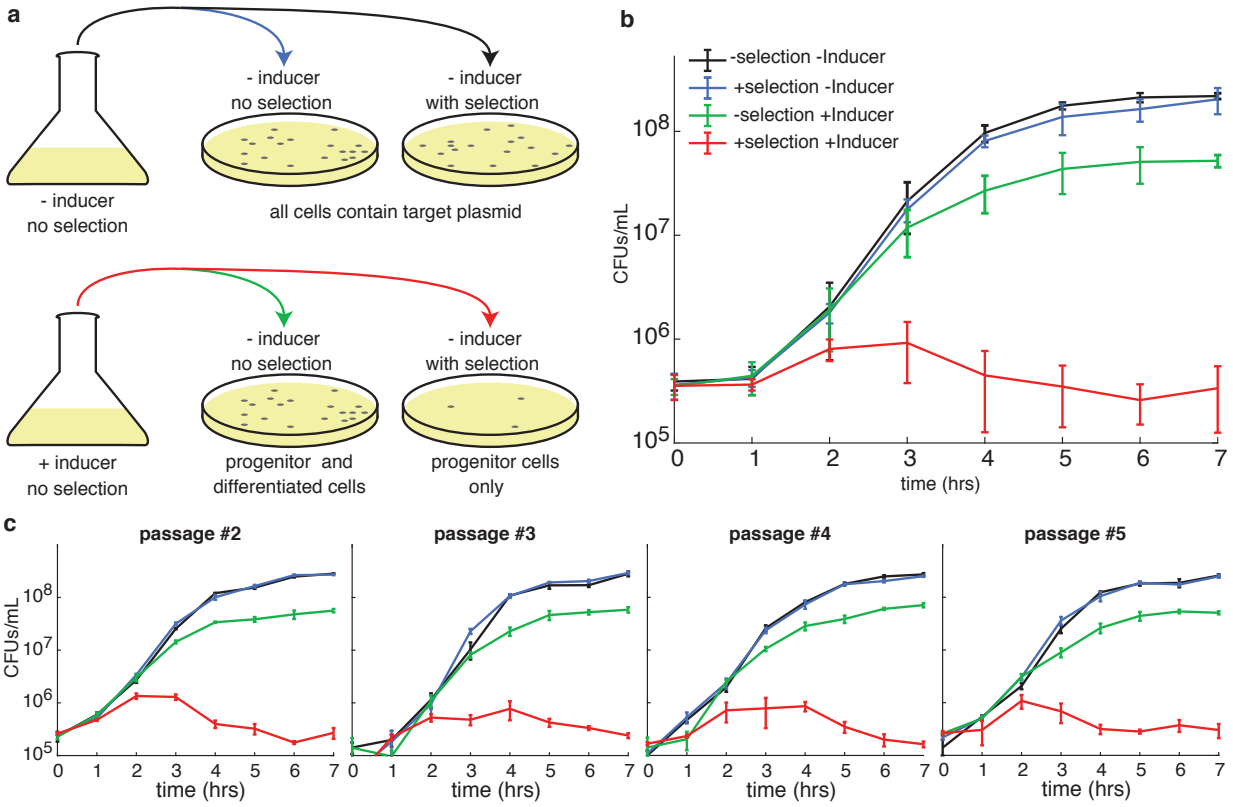

Figure 2 Progenitor cells can undergo multiple rounds of APP. **(a)** Pictorial description of the plating assay. Liquid cultures without (top) and with (bottom) inducer were plated onto agarose with and without selection for the target plasmid. Without inducer (top) the number of CFUs should be the same independent of the antibiotic. With inducer, however, only progenitor cells will grow on the plate that includes antibiotic. **(b)** CFUs as a function of time for each of the four conditions described in (a). In the case of the uninduced culture (black and blue lines) there is almost no difference between cells plated with or without chloramphenicol. For the induced culture (green and red lines), however, only the cells plated without chloramphenicol show normal growth (green line), whereas the number of cells able to grow on chloramphenicol (progenitor cells) remain roughly constant over time. **(c)** To prove that the progenitor cells still contain the intact APP system after a cycle of induction, we picked a cell from the induced culture plated on chloramphenicol 7h after the induction (last point of the red curve) and reinoculated it overnight to repeat the plating assay. The colony was able to provide nearly identical behavior in every sequential re-inoculation. Error bars represent standard deviation.

blue curves). The results were very different, however, when arabinose was included in the liquid culture. In that case, CFU counts were near the uninduced counts when plated onto plates lacking chloramphenicol. This is expected, as both cells with (progenitor cells) and without (daughter cells) the target plasmid should grow normally (Fig. 2b, green curve). When plated onto selective plates, however, CFU counts were drastically lower (Fig. 2b, red curve). This is consistent with the majority of cells having undergone differentiation via APP: only cells that kept the nucleoprotein complex can grow while those that lack it cannot.

To confirm the loss of target plasmid is solely due to the accumulation of ParB protein, we induced APP when applied to target plasmid with a mutated *parS* domain and observed a negligible loss of target plasmid (Fig. S4). We also observed a reduction in overall CFU counts when the APP network is fully induced at 0.2% arabinose, suggesting a non-negligible fitness cost associated with induced CFP::ParB expression (Fig. 2b). For all the experiment not involving single cell microscopy, we switched to CFP::ParB to free up sfYFP for later microscopy experiments (see below), however, both CFP::ParB and sfYFP::ParB behaved similarly in our assays (Fig. S4).

We next tested the robustness of our system by performing multiple cycles of induced APP in sequence. To do this, we picked and regrew a colony from a 7-hour plate with chloramphenicol with cells from the induced culture (the rightmost point of the red curve in Fig. 2b). On this plate all cells should be progenitor cells and have both plasmids of the APP system. On the following day, we repeated the above process of induction of APP and plating. CFU counts for each case were similar to those obtained with the first induction, as were those on subsequent repetitions of the experiment (Fig. 2c). This means that even after a round of APP, the progenitor cells were able to recover and undergo subsequent rounds of APP.

To further confirm that the target plasmid is lost in differentiated cells, we picked 12 colonies from the induced population plated without chloramphenicol (where the majority of cells

are expected to have lost the target plasmid) and measured the amount of target plasmid DNA using qPCR. They were all positive for the presence of the regulatory plasmid but all show no amplification of the target plasmid for the first 30 cycles of amplification in the qPCR reaction (data not shown). Moreover, no colony grew on chloramphenicol-containing LB but all of them grew on plates lacking chloramphenicol. We also analyzed the plasmid content of both induced and uninduced populations using qPCR in order to examine the dynamics of APP in the growing populations. As shown in Fig. S3, the ratio of target plasmid (segregating asymmetrically) to the regulatory plasmid (segregating symmetrically) decreases over time in the induced population. In contrast, the uninduced population shows a roughly constant ratio of the two plasmids over time.

Tuning the efficiency of APP

We next explored potential strategies for tuning ligand inducible APP. To do this, we tested two other versions of the target plasmid that contain different origins of replication (pUC and pSC101) in addition to the original version containing pMB1. The pUC origin of replication is a mutant pMB1 that confers a much higher copy number (~300-500 copies per cell[45]) compared to wild type (~10-20 copies per cells[46]). We specifically wanted to know if a target plasmid with a high copy number would aggregate and segregate as efficiently as the one with the pMB1 origin. The pSC101 origin confers a low copy number (~5 copies per cell) and is actively partitioned by ParA of *E. Coli's* SMC complex[47]. We wanted to know if the active segregation mechanism of pSC101 would interfere with the APP systems ability to aggregate the target plasmid. All three versions of the target plasmids were then tested with various amounts of inducer. As shown in Figs. 3a,c,e, the fraction of progenitor cells (as measured by the plating assay) decrease with increasing inducer concentration. Further, the partitioning of target

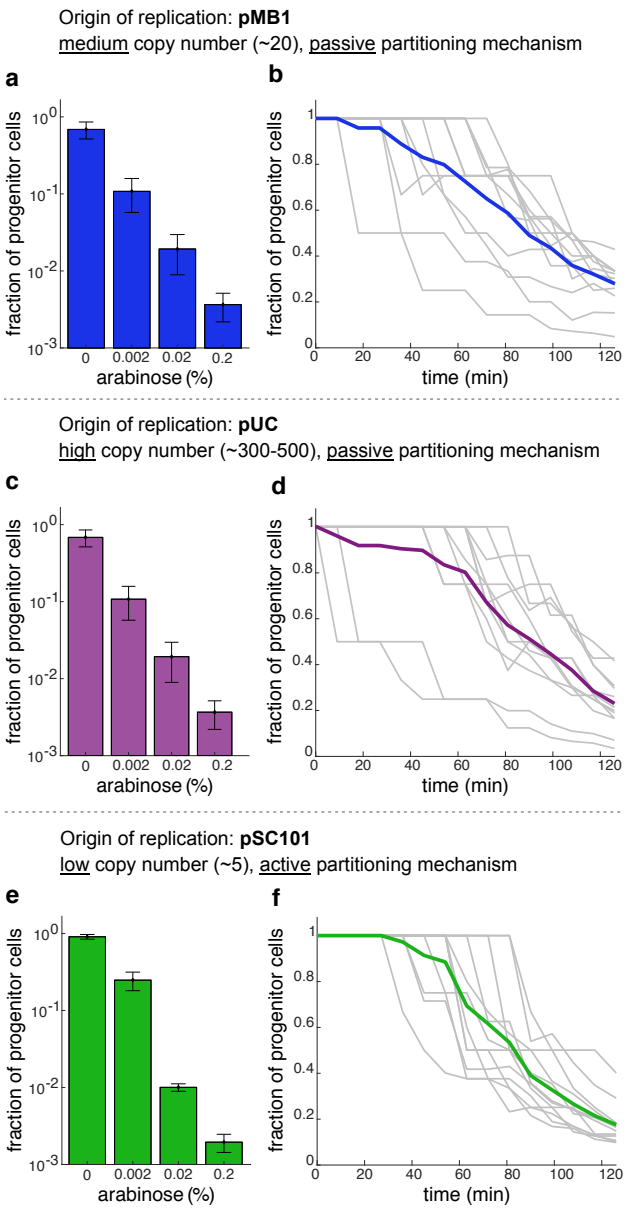

Figure 3 APP with different plasmid origins. **(a)** Fraction of progenitor cells as a function of inducer concentration using a target plasmid with the pMB1 origin of replication as measured by a plating assay. Results show that the efficiency of APP can be modulated by varying the amount of inducer. **(b)** Fraction of progenitor cells in an induced colony as a function of time as measured by single-cell fluorescence microscopy. Each colony started as a single progenitor cell. Shown are individual experiments (grey lines) and the mean (colored line). **(c, d)** Same as (a, b), but with the pUC origin on the target plasmid. **(e, f)** Same as (a, b), but with the pSC101 origin on the target plasmid. Error bars represent standard deviation.

plasmid was robust to the changes in copy number and active segregation mechanism conferred by the pUC and pSC101 origins.

We further investigated the effect of target plasmid copy number though single cell microscopy for each version of the target plasmid (shown in Figs. 3b,d,f) to determine if the dynamics of plasmid loss differed among the three origins of replication. To do this, we used fluorescence microscopy to follow the growth of a single cell in an LB agar pad perfused with 0.2% arabinose and ampicillin. We calculated the fraction of progenitor cells (recognized by the presence of the fluorescent punctum) in the growing population as a function of time. As can be seen in Figs. 3b,d,f, the dynamics of each population (i.e. the fraction of cells containing target plasmid as a function of time) were similar for each of the three origins of replication.

An orthogonal APP system for the engineering of pluripotent bacterial stem cells

Lastly, we explored the possibility of expanding the potential of APP by refactoring a second orthogonal APP circuit into *E. coli*. Our end goal was to build a circuit capable of independently partitioning two different plasmids upon the induction of two separate *trans*-acting proteins. In this way, one could differentiate an initial isogenic strain into four different cell types. To do this, we first replaced *parB* on the regulatory plasmid with *sopB*, and the *parS* site on the target plasmid with *sopC.* These two elements are from the F plasmid, and have native functions similar to their counterparts[48].

Just as with the ParB/*parS* system, the fraction of progenitor cells decreases in the SopB/*sopC* system as a function of increasing amount of inducer (Fig. 4a), and subsequent rounds of APP were possible, provided the inducer concentration was not too high (Fig. S5). We next assessed the orthogonality of the two networks by comparing the results all the four possible combinations of the two plasmid-gathering proteins and two cis-acting sequences (Fig.

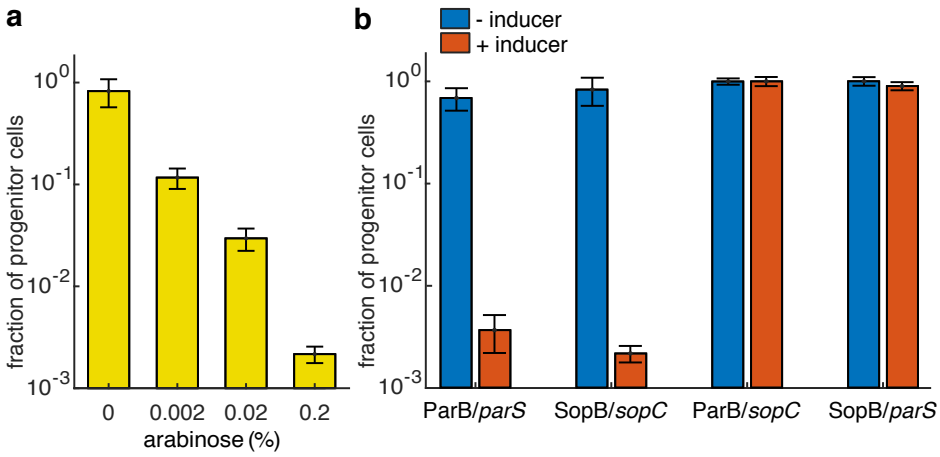

Figure 4 An orthogonal system for APP. **(a)** Fraction of progenitor cells as a function of arabinose using the SopB/*sopC* system as measured by the plating assay. **(b)** Fraction of progenitor cells for induced (red) and uninduced (blue) cultures as measured by the plating assay. Each combination of protein and binding site were tested. APP occurred when the protein and binding site came from the same system (left two) and not when they came from different systems (right two). Error bars represent standard deviation.

4b). Only the correct pairing of the APP network elements resulted in APP, whereas the mispaired combinations ParB/*sopC* and SopB/*parS* did not.

To construct the pluripotent APP circuit, we combined the two synthetic APP pathways together by refactoring the four genetic elements into a new circuit made of three plasmids: two target plasmids (each containing one of the two centromere-like sequences, *parS* and *sopC*) with chloramphenicol and spectinomycin resistance, and a regulatory plasmid with *parB* and *sopB* being driven by arabinose and IPTG inducible promoters, respectively (Fig. 5a). With this new circuit, the progenitor cells can differentiate in several ways (Fig. 5b). If either inducer is used alone, progenitor cells should begin to produce one of two partially differentiated cell types that lack one of the target plasmids. If both inducers are used simultaneously, progenitor cells produce terminally differentiated cells lacking both target plasmids. Finally, if one sequentially induces the system with first one inducer and then the other, partially differentiated cells should begin to produce terminally differentiated cells.

We again used the plating assay to assess the amount of differentiation of the pluripotent circuit after we induced it with one of the two inducers, or both (Fig. 5c). For this plating assay, the resulting cultures were plated after 7 hours onto agarose with various selective antibiotics (ampicillin (A), ampicillin and spectinomycin (AS), ampicillin and chloramphenicol (AC), or ampicillin, chloramphenicol, and spectinomycin (ASC)) to select for various combinations of plasmids. In each case, the fraction of progenitor cells matched expectations: e.g. when only arabinose was used to induce, most cells grew only on ampicillin or ampicillin plus spectinomycin, as the target plasmid containing conferring chloramphenicol resistance had been lost in the majority of cells.

The above results can also be seen through fluorescence microscopy (Fig. 5e). In the absence of inducer, cells contain both red and yellow fluorescence (top row). However, if one of the inducers is present, the number of cells with the corresponding fluorescence is drastically

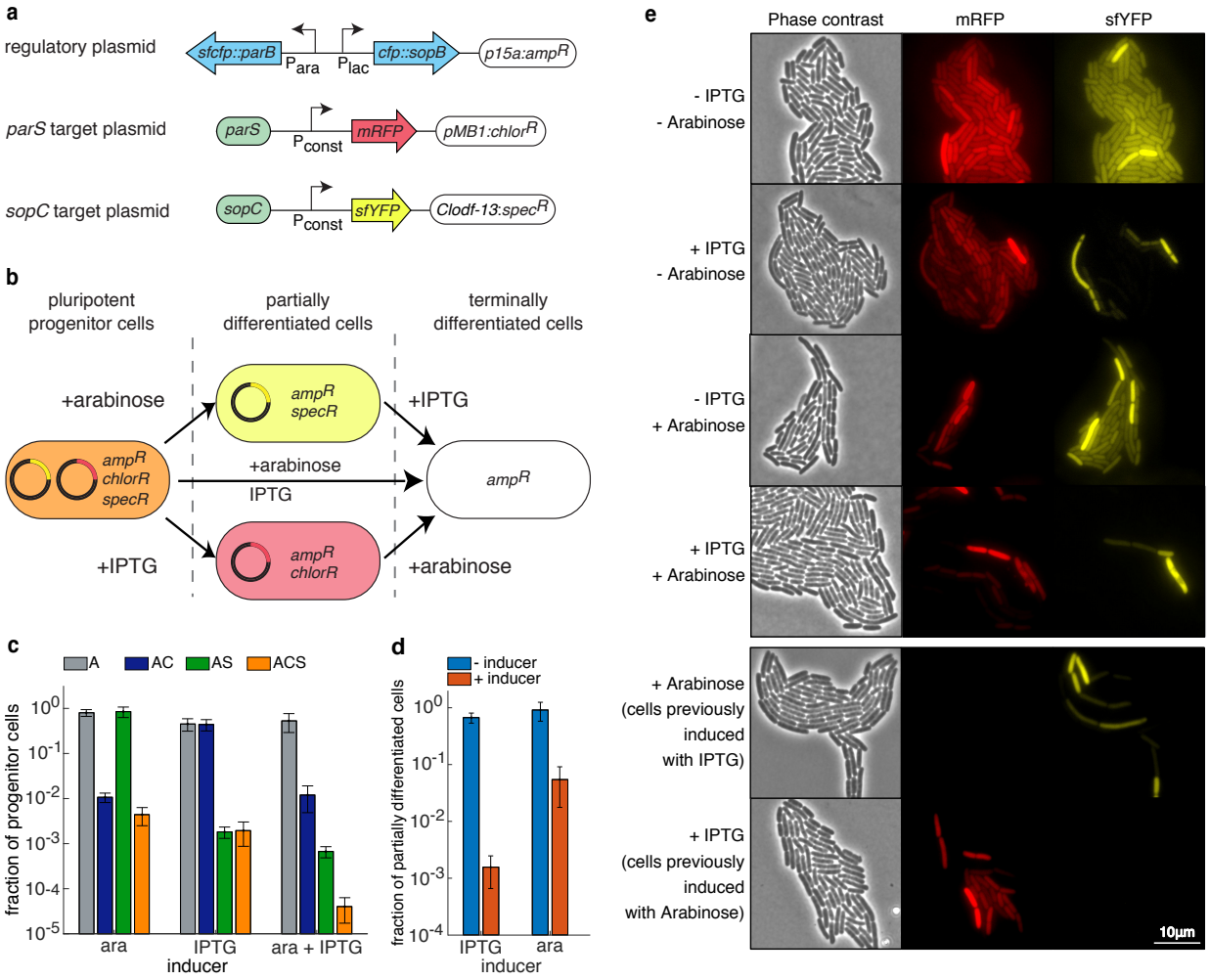

Figure 5 A pluripotent bacterial stem cell. **(a)** Schematics of key elements on each of the three plasmids used in the pluripotent bacterial stem cell. **(b)** Diagram of possible differentiation routes for the pluripotent progenitor cells. Depending on the inducers, progenitor cells can lose either one of the target plasmids, or both. **(c)** Fraction of progenitor cells in different antibiotic conditions for different combinations of the inducers, as measured by the plating assay (A – ampicillin; C – chloramphenicol; S – spectinomycin). When induced with just arabinose, chloramphenicol resistance is lost. When induced with just IPTG, spectinomycin resistance is lost. When induced with both arabinose and IPTG, both spectinomycin and chloramphenicol resistances are lost. **(d)** Fraction of partially differentiated cells (as measured by the plating assay) with (red) and without (blue) induction of the remaining APP system. In both cases, the remaining APP system retains its ability to differentiate. **(e)** Phase (left), red fluorescence (middle), and yellow fluorescence (right) images of cells after induction with various combinations of inducers. Also shown (bottom two rows) are colonies previously induced for differentiation of one pathway undergoing induction for the other pathway. Error bars represent standard deviation.

reduced (second and third rows). If both inducers are present, the resulting population is primarily empty of either fluorescent protein. Note that in each case, there are still progenitor cells present in the culture, indicative of the asymmetric nature of the differentiation. These results also hold for sequential induction, as displayed in the bottom two rows of Fig. 5e.

Discussion

In this work, we have developed a novel synthetic gene circuit for creating pluripotent stem cells in *E. coli*. This circuit distinguishes itself from other synthetic differentiation mechanisms, especially toggle switches, in several important ways. First, differentiation in our circuit occurs through asymmetric cell division, meaning that a progenitor cell will always remain in the culture, ready to reseed the population. This ability is key to tissue homeostasis in multicellular organisms[49] and our circuit could be combined with intercellular signaling mechanisms to auto-regulate differentiation in a similar manner.

Second, differentiation with the APP circuit is irreversible. Once a plasmid is lost in a daughter cell, it cannot be recovered (barring some form of horizontal gene transfer). This means that no refractory period exists if the circuit was used as a memory device. Once a transient signal has been sent, differentiated cells will appear and begin to proliferate as the environment allows. In contrast, when input signals of a toggle switch are transient, the system will reset to its original state after some time[13]. The only way to reset the APP system is to rid the colony of differentiated cells (by whichever means appropriate) and regrow the progenitor cells.

Finally, one disadvantage of co-repressive toggle switches is that they are difficult to tune because they generally have a limited parameter space in which they exhibit bistability. The iterative nature of constructing such circuits can add a significant amount of time to the design/build/test cycle[50]. The APP system, though, requires very little tuning, as differentiation

requires only the accumulation of the DNA binding protein and not the repression of another transcriptional state. Hence, the balance of two nonlinear processes is unnecessary. This, and the other advantages noted above, make the APP system a great option for creating differentiated multicellular systems from simple prokaryotic hosts.

Methods

Plating assay – growth curve: Cells of *E. coli* strain JS006-ALT containing both the regulatory plasmid and the target plasmid were cultured overnight at 37˚C shaking at 200rpm in LB media containing both ampicillin (Amp, 100μg/mL) and chloramphenicol (Cm, 34μg/mL) antibiotic. Two 250mL Erlenmeyer flasks containing 50mL of LB media with only Amp were inoculated with overnight culture at 0.1% v/v and incubated at 37˚C shaking at 200rpm for up to 8 hours. At 1 hour post inoculation, inducer was added to one of the two cultures – this is what we define as 'time 0'.

Starting from time 0, the growing culture was sampled every hour. At each sampling, culture was diluted into non-selective LB media and then plated on to two sets of LB agar plates: One set of plates contained only Amp, to assay the total CFU count, and the other set contained both Amp+Cm, to assay the CFU count associated with cells containing target plasmid. 100μl of each final culture dilution was applied and spread on to each plate using 12 glass beads (Millipore Sigma).

For each time point, culture from each flask was diluted at specific dilution ratio that depended on the presence or absence of inducer and on what antibiotic was present in the LB-agar. For cultures with no added inducer that were plated on solid media plated with or without Cm, and for cultures with added inducer that were plated on solid media without Cm, the dilution ratios are as follows: time 0h: 1/1000; time 1h: 1/2000; time 2h: 1/10000; time 3h: 1/100000;

time 4h: 1/200000; time 5-6-7h: 1/500000. For cultures with added inducer that were plated on solid media containing Cm, the dilution ratios are as follows: time 0: 1/1000; time 1h: 1/2000; time 2-3-4-5-6-7h: 1/10000.

For each plate, 12 glass beads were applied to each plate to spread 100μl of final diluted cell culture. Plates were then incubated at 37˚C until colonies reached at least 0.5mm in diameter. Plates were then imaged through Alpha Innotech Multiimage™ light cabinet using AlphaView Fluorchem FC3 (version 3.4.1). Total CFUs on each plate were counted with imageJ (version 2.0.0-rc-54/1.51g).

All plating assays follow the protocol described above. If only one time point is shown, it is the 7hr post induction timepoint.

APP titration assay: Cells were inoculated from overnight culture as described in 'plating assay' into four different flasks. At 1hr post inoculation (time 0 in Figure 3) each flask was added with the stated amount of L-arabinose (Millipore Sigma): 0%, 0.002%, 0.02% and 0.2% m/V. 7 hours after induction, cultures were diluted and plated as described in 'plating assay'. Dilutions for the ParB/*parS* system: For cultures with no added inducer that were plated on solid media plated with or without Cm, and for cultures with added inducer that were plated on solid media without Cm, the dilution factor was 1/500000. For cultures with added inducer that were plated on solid media containing Cm, the dilution factor was 1/100000 for cultures induced with 0.002% arabinose, 1/100000 for cultures induced with 0.02% arabinose, 1/10000 for cultures induced with 0.2% arabinose. Dilutions for the SopB/*sopC* system: For cultures with no added inducer that were plated on solid media plated with or without Cm, and for cultures with added inducer that were plated on solid media without Cm, the dilution factor was 1/500000. For cultures with added inducer that were plated on solid media containing Cm, the dilution factor was 1/100000

for cultures induced with 0.002% arabinose, 1/10000 for cultures induced with 0.02% arabinose, and 1/1000 for cultures induced with 0.2% arabinose.

APP orthogonal system plating assay: Cells were inoculated from overnight culture as described in 'plating assay' into four different flasks. At 1hr post inoculation (time 0 in Figure 3), each flask was added with either no inducer, 0.2% arabinose, 0.1mM IPTG or 0.2% arabinose and 0.1mM IPTG. 7 hours after addition of inducer, cultures were diluted and plated on to four different sets of plates: Amp, Amp+Cm, Amp and spectinomycin (Spec, 50μg/mL), or Amp+Cm+Spec. The culture with no added inducer was diluted 1/500000 for each plating condition. The culture with 0.2% arabinose was diluted 1/500000 when plated on Amp or Amp+Spec and was diluted 1/10000 when plated on Amp, Amp+Cm, or Amp+Cm+Spec. The culture induced with 0.1mM IPTG was diluted 1/500000 when plated on Amp, or Amp+Cm, and diluted 1/1000 when plated on Amp+Spec, or Amp+Cm+Spec. Plates were incubated at 37 ˚C until colonies grew to about 0.5mm in diameter and were imaged as described in 'plating assay'.

Single cell Microscopy Assay: We imaged cells incubated underneath a layer of solid LB -agar (1.5% agar, 1-2mm). 1uL of cell culture was placed under a slab LB-agar were placed within a 50mm glass cover slip bottomed petri dish with 30mm Glass Diameter (MatTek Corporation). Images have been acquired using an inverted fluorescence microscope and imaged every 3min (Nikon).

qPCR: Cells were inoculated from overnight culture as described in 'plating assay', into two different flasks. At time 0, one hour after the initial inoculation, one flask was induced with 0.2% L-arabinose. Starting at time 0, We sampled each flask every hour. We extracted the following volumes at each time point: time 0h: 20mL; time 1h: 20mL; time 2h: 10mL; time 3h: 5mL; time

4h: 3mL; time 5h, 6h, 7h: 1mL. Cells were pelleted and plasmid DNA was extracted with the QIAprep Spin Miniprep Kit at a final elution volume of 50μL. For the qPCR reaction, we used 1μL of the DNA resulting from the mini-prep. Forward and reverse primers were added to a final total primer concentration of 0.1μM in addition to 5μL of Maxima SYBR Green/ROX qPCR Master Mix (Thermofischer Scientific). Nuclease free water was added for a final reaction volume of 10μL. A Bio-Rad CFX96 qPCR machine was used for data collection using the following PCR program: 50 °C for 2 min, 95 °C for 10 min, followed by 30 cycles of 95 °C for 15 s and 60 °C for 1 min. All of the measurements were followed by melting curve analysis. Results were analyzed using Bio-Rad qPCR analysis software by a relative standard curve. For quantification, a 5-point standard curve covering a 10^4-fold range of concentrations of the target plasmid and the regulatory plasmid was run in parallel and used to determine the relative DNA abundance in each sample. It was shown that the qPCR primers for both the target and regulatory plasmid had a primer efficiency between 82.73–93.22%. All of the DNA samples were measured in triplicate, and non-template controls run in parallel to control for contamination and nonspecific amplification or primer dimers. Melting curve analysis was performed to confirm that only a single product was amplified.

The primers used for qPCR in this study were:

Target Plasmid FWD: 5'- GCCGGAAATCGTCGTGGTATTC - 3'

Target Plasmid REV: 5'- CAATGAAAGACGGTGAGCTGGTG - 3'

pSM015 Plasmid FWD: 5'- CGTCGTTTGGTATGGCTTCATTCAG - 3'

pSM015 Plasmid REV: 5'- CTAACCGCTTTTTTGCACAACATGG - 3'

qPCR on individual colonies (colonies): We collected cells from the induced culture plated without Cm, 7h after adding L-arabinose as described in 'plating assay'. Single colonies of the

plate were picked and resuspended in 10μL of PBS. Following the same protocol as descried in above, 1μL of the cell resuspension was used for each reaction.

Acknowledgements

We are especially grateful to Lucy Shapiro and Christine Jacobs-Wagner for providing plasmids. This work was funded by the Defense Advanced Research Projects Agency (DARPA) Biological Technologies (BTO) Biological Controls Program, award #HR0011-17-2-0012 (approved for public release; distribution is unlimited) (MRB and OAI); the National Science Foundation through grant MCB-1616755 (OAI) and through the joint NSF-National Institute of General Medical Sciences Mathematical Biology Program grant DMS-166290 (MRB); the Welch Foundation grant C-1729 (MRB); and the National Institutes of Health grant R01GM117138 (MRB).

Author Contributions

MRB, OAI, and SM conceived of the study. SM and DS performed experiments and analyzed data. MRB, OAI, and JC oversaw the project. All authors wrote the manuscript.

References

1. Hasty, J., McMillen, D. & Collins, J. J. Engineered gene circuits. *Nature* **420,** 224–230 (2002).
2. Sprinzak, D. & Elowitz, M. B. Reconstruction of genetic circuits. *Nature* **438,** 443–448 (2005).
3. Gardner, T. S., Cantor, C. R. & Collins, J. J. Construction of a genetic toggle switch in Escherichia coli. *Nature* **403,** 339–342 (2000).

4. Stricker, J. *et al.* A fast, robust and tunable synthetic gene oscillator. *Nature* **456,** 516–519 (2008).

5. Basu, S., Gerchman, Y., Collins, C. H., Arnold, F. H. & Weiss, R. A synthetic multicellular system for programmed pattern formation. *Nature* **434,** 1130–1134 (2005).

6. Weber, W. & Fussenegger, M. Emerging biomedical applications of synthetic biology. *Nature Reviews Genetics* **13,** 21–35 (2012).

7. Danino, T., Lo, J., Prindle, A., Hasty, J. & Bhatia, S. N. In Vivo Gene Expression Dynamics of Tumor-Targeted Bacteria. *ACS Synth. Biol. 1 465-470 OCT 2012* **1,** (2012).

8. Weber, W. & Fussenegger, M. The impact of synthetic biology on drug discovery. *Drug Discov. Today* **14,** 956–963 (2009).

9. Zhang, F., Carothers, J. M. & Keasling, J. D. Design of a dynamic sensor-regulator system for production of chemicals and fuels derived from fatty acids. *Nat. Biotechnol.* **30,** 354–359 (2012).

10. Dietrich, J. A., Shis, D. L., Alikhani, A. & Keasling, J. D. Transcription factor-based screens and synthetic selections for microbial small-molecule biosynthesis. *ACS Synth. Biol.* **2,** 47–58 (2013).

11. Lu, T. K. & Collins, J. J. Engineered bacteriophage targeting gene networks as adjuvants for antibiotic therapy. *Proc. Natl. Acad. Sci.* **106,** 4629–4634 (2009).

12. Xie, Z., Wroblewska, L., Prochazka, L., Weiss, R. & Benenson, Y. Multi-input RNAi-based logic circuit for identification of specific cancer cells. *Science (80-.).* **333,** 1307–1311 (2011).

13. Kotula, J. W. *et al.* Programmable bacteria detect and record an environmental signal in the mammalian gut. *Proc. Natl. Acad. Sci.* **111,** 4838–4843 (2014).

14. Masiello, C. A. *et al.* Biochar and Microbial Signaling: Production Conditions Determine Effects on Microbial Communication. *Environ. Sci. Technol.* **47,** 11496–11503 (2013).

15. Levskaya, A. *et al.* Engineering Escherichia coli to see light. *Nature* **438,** 441–442 (2005).

16. Sohka, T., Heins, R. A. & Ostermeier, M. Morphogen-defined patterning of Escherichia coli enabled by an externally tunable band-pass filter. *J. Biol. Eng.* **3,** (2009).

17. Basu, S., Mehreja, R., Thiberge, S., Chen, M.-T. & Weiss, R. Spatiotemporal control of gene expression with pulse-generating networks. *Proc. Natl. Acad. Sci. U. S. A.* **101,** 6355–60 (2004).

18. Payne, S. *et al.* Temporal control of self-organized pattern formation without morphogen gradients in bacteria. *Mol. Syst. Biol.* **9,** 1–10 (2013).

19. Danino, T., Mondragón-Palomino, O., Tsimring, L. & Hasty, J. A synchronized quorum of genetic clocks. *Nature* **463,** 326–330 (2010).

20. Prindle, A. *et al.* A sensing array of radically coupled genetic 'biopixels'. *Nature* **481,** 39–44 (2012).

21. Chen, Y., Kim, J. K., Hirning, A. J., Josić, K. & Bennett, M. R. Emergent genetic oscillations in a synthetic microbial consortium. *Science (80-.).* **349,** 986–989 (2015).

22. You, L., Cox, R. S., Weiss, R. & Arnold, F. H. Programmed population control by cell-cell communication and regulated killing. *Nature* **428,** 868–871 (2004).

23. Yamanaka, K. T. and S. Induction of Pluripotent Stem Cells from Mouse Embryonic and Adult Fibroblast Cultures by Defined Factors. *Cell* **126,** 663–676 (2006).

24. Narula, J., Devi, S. N., Fujita, M. & Igoshin, O. A. Ultrasensitivity of the Bacillus subtilis sporulation decision. *Proc. Natl. Acad. Sci.* **109,** E3513–E3522 (2012).

25. Cairns, L. S., Hobley, L. & Stanley-Wall, N. R. Biofilm formation by Bacillus subtilis: New insights into regulatory strategies and assembly mechanisms. *Molecular Microbiology* **93,** 587–598 (2014).

26. Narula, J. *et al.* Chromosomal Arrangement of Phosphorelay Genes Couples Sporulation and DNA Replication. *Cell* **162,** 328–337 (2015).

27. Higgins, D. & Dworkin, J. Recent progress in Bacillus subtilis sporulation. *FEMS Microbiology Reviews* **36,** 131–148 (2012).

28. Lopez, D., Vlamakis, H. & Kolter, R. Generation of multiple cell types in Bacillus subtilis. *FEMS Microbiology Reviews* **33,** 152–163 (2009).

29. Vlamakis, H., Aguilar, C., Losick, R. & Kolter, R. Control of cell fate by the formation of an architecturally complex bacterial community. *Genes Dev.* **22,** 945–953 (2008).

30. McCarter, L., Hilmen, M. & Silverman, M. Flagellar dynamometer controls swarmer cell differentiation of V. parahaemolyticus. *Cell* **54,** 345–351 (1988).

31. Rather, P. N. Swarmer cell differentiation in Proteus mirabilis. *Environmental Microbiology* **7,** 1065–1073 (2005).

32. Morgenstein, R. M., Szostek, B. & Rather, P. N. Regulation of gene expression during swarmer cell differentiation in Proteus mirabilis. *FEMS Microbiology Reviews* **34,** 753–763 (2010).

33. Ausmees, N. & Jacobs-Wagner, C. Spatial and temporal control of differentiation and cell cycle progression in Caulobacter crescentus. *Annu. Rev. Microbiol.* **57,** 225–247 (2003).

34. Tsokos, C. G. & Laub, M. T. Polarity and cell fate asymmetry in Caulobacter crescentus. *Curr. Opin. Microbiol.* **15,** 744–750 (2012).

35. Atkinson, M. R., Savageau, M. A., Myers, J. T. & Ninfa, A. J. Development of genetic circuitry exhibiting toggle switch or oscillatory behavior in Escherichia coli. *Cell* **113,** 597–607 (2003).

36. Thattai, M. & van Oudenaarden, A. Intrinsic noise in gene regulatory networks. *Proc. Natl. Acad. Sci.* **98,** 8614–8619 (2001).

37. Gupta, C., López, J. M., Ott, W., Josić, K. & Bennett, M. R. Transcriptional delay stabilizes bistable gene networks. *Phys. Rev. Lett.* **111,** (2013).

38. Balázsi, G., Van Oudenaarden, A. & Collins, J. J. Cellular decision making and biological

noise: From microbes to mammals. *Cell* **144,** 910–925 (2011).

39. Egbert, R. G. & Klavins, E. Fine-tuning gene networks using simple sequence repeats. *Proc. Natl. Acad. Sci. U. S. A.* **109,** 16817–22 (2012).

40. Toro, E., Hong, S. H., McAdams, H. H. & Shapiro, L. Caulobacter requires a dedicated mechanism to initiate chromosome segregation. *Proc Natl Acad Sci U S A* **105,** 15435–15440 (2008).

41. Schumacher, M. A. Structural biology of plasmid partition: uncovering the molecular mechanisms of DNA segregation. *Biochem. J* **412,** 1–18 (2008).

42. Li, Y., Dabrazhynetskaya, A., Youngren, B. & Austin, S. The role of Par proteins in the active segregation of the P1 plasmid. *Mol. Microbiol.* **53,** 93–102 (2004).

43. Tran, N. T. *et al.* Permissive zones for the centromere-binding protein ParB on the Caulobacter crescentuschromosome. *Nucleic Acids Res.* **46,** 1196–1209 (2018).

44. Mierzejewska, J. & Jagura-Burdzy, G. Prokaryotic ParA-ParB-parS system links bacterial chromosome segregation with the cell cycle. *Plasmid* **67,** 1–14 (2012).

45. Yanisch-Perron, C., Vieira, J. & Messing, J. Improved M13 phage cloning vectors and host strains: nucleotide sequences of the M13mpl8 and pUC19 vectors. *Gene* **33,** 103–119 (1985).

46. Lee, C., Kim, J., Shin, S. G. & Hwang, S. Absolute and relative QPCR quantification of plasmid copy number in Escherichia coli. *J. Biotechnol.* **123,** 273–280 (2006).

47. Meacock, P. A. & Cohen, S. N. Partitioning of bacterial plasmids during cell division: a cis-acting locus that accomplishes stable plasmid inheritance. *Cell* **20,** 529–542 (1980).

48. Schumacher, M. A., Piro, K. M. & Xu, W. Insight into F plasmid DNA segregation revealed by structures of SopB and SopB-DNA complexes. *Nucleic Acids Res.* **38,** 4514–4526 (2010).

49. Simons, B. D. & Clevers, H. Strategies for homeostatic stem cell self-renewal in adult

tissues. *Cell* **145,** 851–862 (2011).

50. Litcofsky, K. D., Afeyan, R. B., Krom, R. J., Khalil, A. S. & Collins, J. J. Iterative plug-and-play methodology for constructing and modifying synthetic gene networks. *Nat. Methods* **9,** 1077–1080 (2012).